Production and Characterization of High Solid Content Cellulose Nanofibrils from Pretreated Fluff Pulp

Prabaharan Graceraj Ponnusamy
University of Georgia
Suraj Sharma
University of Georgia
Sudhagar Mani (smani@uga.edu)
University of Georgia https://orcid.org/0000-0003-1920-8381

Research Article

Keywords: Cellulose nanofibrils. Ball milling. Homogenization. Solid content. Crystallinity. Thermal stability

Posted Date: December 22nd, 2021

DOI: https://doi.org/10.21203/rs.3.rs-1157792/v1

Abstract

The increasing demand for cellulose nanofibrils (CNF) necessitates the development of novel processes to produce high-solid content and consistent quality nanofibrils. In this study, we investigated the combination of mechanical and chemical pretreatment methods (carboxymethylcellulose, CMC dispersion, and sodium hydroxide, NaOH swelling with ball milling) for cellulose fibers followed by high-pressure homogenization to evaluate the CNF characteristics. The carboxymethylcellulose (CMC) dispersion with 75 min ball milling and NaOH swelling with 15, 45, and 75 min ball milling of cellulose slurry reduced the fiber dimensions by up to 90% that eased the fibrillation to produce about 6% solid content CNF during high-pressure homogenization. The characterization of CNF hydrogels produced from pretreated samples revealed that they had an average fibril width of less than 30 nm with good dispersion stability. The CMC dispersion and NaOH swelling with ball milling of cellulose slurry did not significantly affect the chemical structure and the crystallinity of CNF hydrogels. On the other hand, the tensile strength of all the pretreated CNF samples was increased up to 105±14 MPa when compared with that of the control sample (58±6 MPa). NaOH treatment has slightly increased the thermal stability of CNF samples over CMC treated and control samples. In conclusion, short fibers generated by mild alkaline pretreatment with ball milling followed by high-pressure homogenization of cellulose fibers can produce the consistent quality CNF with high solid content and tensile strengths for various industrial applications.

Introduction

Nanocellulose is the nanosized polysaccharide having both amorphous and crystalline cellulose comprised of D-glucose units linked by β-1, 4 glycosidic bonds. It is one of the promising nanomaterials for the development of bio-based and environment-friendly products due to its abundant availability, biocompatibility, biodegradability, and superior material properties such as high aspect ratio, specific area, crystallinity, and tensile strength, and ability to form hydrogen bonding with other materials (Bai et al. 2019; Brigham 2018; Havstad 2020; Lokanathan et al. 2017; Singh et al. 2020; Zhang et al. 2013). The surface modification and functionalization of nanocellulose have expanded its widespread application in various sectors of biomedical, pharmaceutical, food, packaging, electronics, and cosmetics (Abitbol et al. 2016; Liu and Kong 2019; Selvaraj et al. 2021). Therefore, the market demand for nanocellulose has been increasing every year and is projected to be about 6 million metric tons (Cowie et al. 2014). Nanocellulose is produced in various forms and is often related to the source of biomass. Forest wood and plant biomass produce two types of nanocellulose: cellulose nanofibrils (CNF) and cellulose nanocrystals (CNC). In addition, the nanocellulose produced from the synthesis of bacterial microorganisms is bacterial cellulose (BC) often studied in the biomedical fields. The other forms of nanocellulose include tunicate cellulose nanocrystals (t-CNC) and algae cellulose particles (AC) which are isolated from tunicates and algal biomass (Klemm et al. 2011; Moon et al. 2011)

The most common types of nanocellulose, CNF, and CNC and are predominantly produced from forest biomass. CNF/CNCs exist as microfibril bundles in the cell walls of plants and wood. The microfibrils are

connected by many strong interfibrillar hydrogen bonds to form cellulose macrofibres. Nanocellulose with 5 to 30 *nm* width and an aspect ratio greater than 50 are defined as CNF, and with rod-like structure, a width of 3 to 10 nm and aspect ratio less than 50 are defined as CNC according to the standard definition of nanomaterials by Technical Association of the Pulp and Paper Industry (TAPPI) (TAPPI 2017). A single micron-sized cellulose fiber consists of numerous CNC and CNF. They are extracted from biomass resources by chemical, mechanical and enzymatic processes. The acid hydrolysis is most widely followed for the extraction of crystalline CNCs from delignified cellulose pulp and cotton fibers. However, the consumption of acids (64%) and low yield (~50%) poses a great challenge in the commercialization of the CNC manufacturing process (Gu et al. 2015; Peng et al. 2011).

The CNFs are manufactured from wood-based cellulose pulps through mechanical disintegration devices such as disc refiner, homogenizer, ball mill, microfluidizer, and ultrafine grinders (Cheng et al. 2018; Chirayil et al. 2014; Stelte and Sanadi 2009; Zhang et al. 2015). The diluted cellulose pulp slurries were subjected to shear, impact, and cavitation pressure in mechanical processing units to break interfibrillar hydrogen bonds and to isolate nanostructured fibrils. The energy requirement of such processes varied from 12,000 to 70,000 kWh t^{-1}. In addition to high energy consumption, clogging and poor dispersibility of long fibers reduced the fibrilization efficiency of the mechanical devices (Abdul Khalil et al. 2016; Alle et al. 2020; Arantes et al. 2020; Kępa et al. 2019; Turbak et al. 1983). Moreover, the extracted CNFs showed widespread distribution in width (3 to 90 nm) and length (200 to 500 nm) (Li et al. 2015). To reduce the high energy consumption and to ease the fibrilization process, different chemical and mechanical pretreatment methods were investigated to produce CNF (Albornoz-Palma et al. 2020; Pirich et al. 2020). The energy consumption of such manufacturing methods was reduced to the range of 1500 to 500 kWh t^{-1} (Klemm et al. 2011). However, the quality of isolated CNFs was inconsistent due to the poor dispersibility and agglomeration of cellulose in the input slurries.

The cellulose fibers from wood and plant-based resources are more prone to agglomeration and formation of network structure due to more unordered cellulose and cellulose Iα on fibril surface to make them stickier (Lawoko et al. 2006). The agglomerated and network-structured cellulose fibers caused the clogging in the homogenizer valve and reduced fibrillation efficiency for increased cellulose concentration in the input slurry. The chemical pretreatment processes such as chloroacetic acid etherification, carboxymethylation enzymatic hydrolysis, and TEMPO oxidation were studied to modify the surface and structure of cellulose to improve fiber dispersibility during CNF isolation processes (Adsul et al. 2005; Ioelovich and Morag 2011; Saito et al. 2006). These processes consumed a considerable amount of hazardous chemicals and even led to low yield, and increased greenhouse gas emissions (Arvidsson et al. 2015; Li et al. 2013).

The mechanical processes such as valley beater and PFI mill were also used to refine and improve dispersibility (Bilodeau and Paradis 2018; Turbak et al. 1983). The cellulose slurry with the concentration of 1.0 and 1.5% was able to disperse in the PFI mill and Valley beater respectively. But, these pretreatment processes were not efficient in reducing fiber width and length (Hai et al. 2013). The CNF fibrilization from lower concentration cellulose slurry and larger fiber width and length, increased the number of passes

and clogging in a homogenizer and reduced the solid content percentage in CNF hydrogel. The CNF having fibril width of less than100 nm and 1% solid content was manufactured by passing cellulose slurry, 10 times through a grinder after processing 30 and 14 times in a refiner and homogenizer, respectively (Iwamoto et al. 2007; Iwamoto et al. 2005). The CNF hydrogel with lower solid content increases bulk volume and causes transportation and handling issues. Moreover, the widespread distribution of fibril width attribute to inconsistent mechanical and physical properties of products produced from them (Li et al. 2015). Therefore, it is important to develop methods to produce highly dispersible, high solid content, and consistent quality CNFs for industrial applications.

The production of CNF was focused on mechanical fibrillation of long-fiber cellulose fibers into CNF (Stelte and Sanadi 2009; Turbak et al. 1983). An earlier study by Lee and Mani (2016) found that the size reduction of fluff pulp by knife milling process not only reduced the fiber dimensions but also improved the fibrillation process to produce CNF. It was hypothesized that the use of short fibers will ease the mechanical fibrillation process and produce consistent quality CNF without fiber clogging. A further reduction in fiber dimension can be possible by the ball milling process and limited studies in the literature were investigated on the effect of ball milling of cellulose fibers on the production of CNF. In addition, the use of carboxymethylcellulose (CMC) as a dispersing agent to minimize fibril agglomeration was investigated and reported that the $-CH_2COO^-$ groups of anionic CMCs were adsorbed into cellulose fiber surface in the CMC dispersion process. More specifically, when CMC was added, the electrostatic repulsive force was induced between cellulose fibers to move them apart and exert uniformly distributed mechanical disintegration force on cellulose fibers (Fras-Zemljič et al. 2006; Laine 2000). An alkaline treatment by low concentration (2%) sodium hydroxide (NaOH) was used to swell cellulose fibers before the fibrillation process and the resultant CNF exhibited improved thermal stability and dispersibility. The low cell-wall cohesion of swollen cellulose fibers improved the delamination and enabled ease of isolation of fibril from bundles (Cai and Zhang 2005; Klemm et al. 2011; Lee et al. 2018). Therefore, the objectives of this study were to investigate the effects of ball milling with CMC as a dispersing agent and NaOH as a swelling agent followed by high-pressure homogenization of knife milled fluff pulp and to determine the physical and mechanical properties of high-solid content CNFs.

Materials And Methods

Materials

The cellulose powder was manufactured from fluff pulp, procured from a commercial paper mill in Georgia, U.S.A. The dried pulp sheet was reduced using the laboratory heavy-duty knife mill (Retsch SM 2000, Germany) with a 0.25 mm screen and three grinding passes. The three-pass shear cut cellulose powder was dried in an oven for 24 hours and was used as a feedstock for this study. Sodium carboxymethyl cellulose (CMC) (molecular weight (M.W) ~250,000 and degree of substitution 0.9) supplied by Sigma Aldrich was used as a dispersing agent and reagent grade sodium hydroxide (NaOH)

in the form of beads, purchased from Amresco was used as a swelling agent. A standard CNF produced by the University of Maine's pilot plant was purchased and used as a reference sample (Ref.).

CNF Production

The CNFs were fibrillated from three-pass knife milled fluff pulp by the combination of pretreatment methods and high-pressure homogenization process as shown in Fig. 1.

Pretreatment of knife milled cellulose

The knife milled cellulose powder was treated by two different pretreatment methods namely CMC dispersion and NaOH swelling treatment followed by ball milling at various milling times to reduce fiber dimensions. For CMC dispersion treatment, the 10% (w/v) of cellulose slurry in deionized water (DI) was prepared from knife-milled cellulose powder by mixing with 2% (w/w) CMC and heated at 80°C for 2h in a hot magnetic stirrer plate. The CMC dispersed cellulose slurry cooled to room temperature before ball milling treatment. A vibratory ball mill (Retsch GmbH, Germany) having a 50 ml mill-jar and a 25 mm diameter stainless-steel ball was used in this study. About 10 g of CMC treated cellulose slurry was taken in the mill-jar along with the ball and processed at 20 Hz vibration frequency and at various ball milling times as shown in Table 1. The high impact and shear forces by the vibratory motion of mill-jar and ball broke the hydrogen bonds between the cellulose fibers to reduce fiber dimensions. After each treatment, the slurry samples were collected and stored at 4° C in a container for the homogenization process. The CMC treated sample without ball milling was chosen as a control sample.

For NaOH treatment, about 10% (w/v) cellulose slurry was prepared from the cellulose powder and was soaked with 2% (w/v) NaOH aqueous solutions at 4°C for 24h. After the treatment, the swollen cellulose was neutralized with acetic acid and washed in DI water to remove excess NaOH as similar to the procedure described by Lee et al., (2016). The neutralized cellulose slurry was ball milled at various ball milling times as listed in Table 1. After each treatment, the treated sample was stored at 4° C for a high-pressure homogenization process. Each treatment was repeated three times. A sub-sample of the treated fibers was sent for fiber dimension measurement.

Table 1
Experimental plan for different pretreatment conditions

Sample ID	Dispersion / swelling agents	Ball mill treatment time (min)	Remarks
0MC	2% CMC (w/w of knife milled cellulose powder)	0	Control sample
15MC		15	Type 1-test samples
45MC		45	
75MC		75	
15MN	2% NaOH in aqueous solution	15	Type 2-test samples
45MN		45	
75MN		75	

CNF fibrilization process

The pretreated cellulose slurries were homogenized using a high-pressure homogenizer (APV-1000, SPXFLOW, U.S.A) at 700 bar pressure. A positive displacement pump in the homogenizer circulated the cellulose slurry through a ceramic homogenizer valve at high pressure. The strong turbulence and cavity pressure generated at the homogenizer valve disrupted the intra and inter-molecular hydrogen bonds of micro cellulose fiber bundles and caused the fibrillation. Preliminary studies have revealed that when the cellulose fibers after CMC and NaOH treatments were subjected to ball milling, the reduction in fiber dimensions enabled to increase the slurry concentration up to 3% (w/v). A further increase in slurry concentrations beyond 3% caused both clogging and ineffective fibrillation of fibers. Thus, the cellulose slurry with 3% concentration was optimal to process in the homogenizer for all experimental conditions except for the control sample as shown in Table 1. For the control treatment, about 1% (w/v) concentration of knife milled cellulose slurry along with 2% CMC was applied. Increasing the cellulose concentration beyond 1% on the control treatment caused the clogging of the homogenizer valves and ceased the operation due to the entangled fiber networks. For each treatment, about 200 ml of cellulose slurry with predefined concentration was passed through a high-pressure homogenizer up to seven cycles to obtain a stable CNF hydrogel. The initial temperature of the cellulose slurry from 25° C reached up to 80° C at the end of the homogenization process. Finally, the homogenized hydrogel was centrifuged (5430 R Centrifuge, Eppendorf, Germany) at 6000 rpm at room temperature for 20 min to remove excess water from CNF hydrogel and the total solid content in the sample was measured. The CNF samples were stored in a refrigerator at 4° C for characterization studies. Each test was repeated three times.

Optical microscope imaging

The dimensions of control and ball mill pretreated cellulose slurries were measured on a DMLS2 optical microscope (Leica Microsystems, Germany). The samples were suspended in distilled water with 0.2% concentration and a drop was placed between the glass slide and coverslip. The images were captured

for the magnification-20x, gain-1.0, and exposure time-100 ms. The length and width of fibers were measured using ImageJ software for analysis (Nechyporchuk et al. 2015; Vanderghem et al. 2012).

Total Solid content

The total solid content of the CNF was determined by drying the CNF samples in a convection oven. The oven temperature was set at 100 ± 5°C. A known amount of CNF sample was weighed ($\varvec{W}_{\varvec{i}}$) and dried in the oven for about 12 hrs or until no change in the dried sample weight. The dried CNF sample was taken out and weighed ($\varvec{W}_{\varvec{f}}$) to determine the total solid content using the following equation (1). Each test was repeated three times.

$$Total\ solid\ content\ (\%) = \frac{W_f}{W_i} \times 100 \quad \ldots\ldots\ldots\ldots\ldots\ldots\ldots\ldots\ldots (1)$$

$Where$

$W_f = Weight\ of\ CNF\ sample\ after\ drying$

$W_i = Weight\ of\ CNF\ sample\ before\ dryiing$

Zeta potential

The Zeta potential values of CNF samples were determined by the electrophoretic light scattering (ELS) technique employed in the NanoBrook 90Plus zeta instrument (Brookhaven Instruments Corporation, U.S.A). A solid-state laser with 35 mW and 660 nm wavelength was used as a light source. The CNF sample suspension with 0.1 wt.% concentration was used for the measurement of 5 sequential readings with four replications.

Fourier-transformed infrared spectra (FTIR)

The chemical structure of CNF samples was characterized by FTIR spectra. The CNF films were manufactured by the film casting method and dried in a desiccator for 24 h before FTIR spectra measurements. The FTIR spectra for each sample were collected in absorbance mode using a Nicolet 6700 VariGATRTM spectrometer (Thermo Electron Corporation, U.S.A.). The CNF films were scanned with a resolution of 4 cm^{-1} in the range of wavenumbers from 4000 to 600 cm^{-1} and each test was triplicated.

X-ray diffraction (XRD)

The crystalline structure of CNF samples was studied by the D8 Advance model XRD system (Bruker, U.S.A) having X-ray source-Co tube and wavelength-1.79037 Å. The system was operated at 35kV voltage and 40mA amperage. Three replications from each sample were analyzed for diffraction angle (2θ) in the range of 10 to 40° and with the rate of 6°/min. The crystallinity index (CI) was calculated from crystalline peaks corresponding to the crystalline and amorphous regions as defined by International Center for Diffraction Data (ICDD) and using the following relationship for three replications (Morais et al. 2013a; Segal et al. 1959).

$$CI = \frac{I_{002} - I_{am}}{I_{002}} \times 100 \quad \text{..... (2)}$$

I_{002}
$= Peak\ intensity\ corresponding\ to\ crystalline\ region\ for\ 2\theta\ between\ 26°\ and\ 27°$

I_{am}
$= Peak\ intensity\ corresponding\ to\ amorphos\ region\ for\ 2\theta\ between\ 21°\ and\ 22°$

Scanning electron microscope (SEM) imaging

The SEM images of CNF films were used to determine the width distribution of CNF samples manufactured. The CNF films were coated with gold-palladium in Leica Mikrosysteme GmbH sputtering unit (coating thickness: 15 nm). The images were obtained from Thermo Fisher Scientific (FEI) Teneo (Thermo Fisher Scientific, Hillsboro, OR, USA), a field emission scanning electron microscope with an accelerating voltage of 5kV and spot size of 8 nm for three replications.

Thermal degradation analysis

The thermogravimetric analysis (TGA) was performed to study the thermal degradation behavior of CNF samples. The SDTA851e thermogravimetric analyzer (Mettler Toledo, U.S.A.) and STARe data analysis software were used to determine the thermal degradation temperature of each sample. The CNF samples were heated in the range of 25 to 600°C with a rate of 10°C/min under an inert atmosphere of nitrogen and with a gas flow of 50 mL/min. The sample mass between 5 to 9 g was used.

Tensile test

The tensile properties of CNF films were determined by the film cast method. The dried CNF films were conditioned at 23° C and 50% RH for 24 h in a desiccator before tensile testing. The tensile tests were performed according to the ASTM D882 (Standard Test Method for Tensile Properties of Thin Plastic Sheeting). Five replications from each CNF sample were tested. An AGS-X tensile tester (Shimadzu, Japan) with a 1 kN load cell was used at 50 mm/min crosshead speed. The tests were performed at ambient temperature. The ultimate tensile strength and Young's modulus were recorded for the analysis.

Statistical analysis

The effect of ball milling time on fiber dimension reduction, solid content percentage, and fibril width was studied by the one-way ANOVA method. The multiple comparison method was also performed to determine which sample mean was different from others. The MATLAB software was used for statistical analysis and tests were conducted for the significance level of 5%.

Results And Discussion

Effects of pretreatment methods on cellulose fiber dimensions

The initial dimensions of both untreated and pretreated cellulose powder were measured using the optical microscope images (Fig. 2). The untreated cellulose powder had an average fiber width of 33±6 μm and length of 309±201 μm. The increase in ball milling time reduced the fiber dimensions with CMC and NaOH treatment as shown in Figs. 2a and 2b. When CMC was used as a dispersing agent to prevent fiber agglomeration, the increase in ball milling time gradually reduced the fiber dimensions. An extensive reduction in fiber dimension was achieved at the ball milling time of 75 min when treated with CMC. On the other hand, when the cellulose fibers were treated with 2% NaOH as a swelling agent, there was a drastic change in the fiber dimension at the ball milling time of 15 min. A further increase in ball milling time did not substantially change the fiber dimensions. During ball milling, the collision of ball media on the treated cellulose fibers exerted repeated impact and shear load on them (Avolio et al. 2012). The continuous impact on cellulose fibers by the ball and mill-jar wall transferred kinetic energy to weak and break off hydrogen bonding and caused the reduction in fiber dimensions (Zhang et al. 2015). Overall, a combination of NaOH treatment with ball milling was effective in reducing the fiber dimensions. The CMC dispersion/NaOH swelling along with ball milling reduced the fiber dimensions (width and length) by up to 90% from the original dimensions. The CMC dispersion with 75 min ball milling and NaOH swelling with 15, 45- and 75-min ball milling treatments reduced the fiber dimensions by 90%. From the large-scale production standpoint, the NaOH swelling with 15 min ball milling would be sufficient to reduce the fiber dimensions to produce CNF.

The one-way ANOVA test showed that there was a significant reduction in cellulose fiber dimensions by the combination of both the pretreatment methods (See the supplementary document - Tables S1 and S2). The multiple comparison test also confirmed that there was a significant change in fiber dimensions between the control and the ball-milled samples (see the supplementary document – Figs S1 and S2). The mean fiber length of pretreated samples was significantly different among all combinations of pretreatments except for the 15MC sample (CMC dispersed and 15min ball milling). The CMC dispersion with ball milling did not significantly change the mean fiber width for 15-min and 45-min ball milling times. However, there was a significant reduction in the mean fiber length of all treatments of CMC dispersed cellulose with ball milling. The hydrogen bonds of cellulose networks were mainly affected by ball mill treatment in the CMC dispersion–ball milling pretreatment method. The swelling of cellulose fiber with NaOH followed by 15 min ball milling significantly reduced the fiber length and width. The cell wall reduction by NaOH swelling made the cellulose fibers more susceptible to weakening the intramolecular hydrogen bonds, thus reducing the fiber width and length even at lower ball milling time. Most cellulose fiber bundles were cleaved by ball milling impacts as shown in Fig. 2c. and 2d to enable efficient dimensional reduction.

Effects of pretreatment methods on the homogenization of cellulose fibers.

A high-pressure homogenizer was used to fibrillate pretreated cellulose slurries into CNF hydrogels. Each pretreatment method determines the concentration of knife-milled cellulose slurries sent to the homogenizer. About 1% knife-milled cellulose slurries with NaOH treatment and without ball milling clogged the homogenizer due to swollen cellulose fibers. However, the CMC dispersed cellulose slurry

without ball mill pretreatment (control sample), was able to pass through the homogenizer with a maximum concentration of 1%. Increasing the cellulose beyond 1% caused pressure fluctuation and clogging of the homogenizer valve. On the other hand, all the pretreated and ball-milled fibers were processed with up to 3% concentration of cellulose slurry in a homogenizer. The turbulence, shear, and cavitation pressures exerted on the cellulose fibers effectively fibrillated the fibers into CNF hydrogels. Increasing the slurry concentration beyond 3%, decreased the pumping ability of the homogenizer and reduced the fibrilization after a few passes of all test samples. It was observed that the increases in ball milling time from 15 min to 75 min did not influence the input slurry concentration beyond 3%.

After each treated sample was homogenized, the CNF hydrogel was centrifuged to remove free water and tested for total solid content (Table 2). The control sample (0MC) produced ~4% solid content CNF due to improved dispersibility during homogenization. The pretreated samples showed a gradual increase in the total solid content of CNF due to reduced fiber dimensions. The CMC treated samples with 15 min and 45 min ball milling (15MC & 45MC) produced only ~4% solid content CNF due to minimal reduction in fiber dimensions (~20%). When the ball milling time was increased to 75 min on the CMC treated fiber (75MC), the total solid content was increased to ~6% due to a drastic reduction in fiber dimensions (~80%). When the cellulose powder was treated with a combination of NaOH and ball milling, the CNF solid content has distinctively changed. The CNF solid content for the treatments 15MN and 45 MN was increased to ~5% due to the fiber dimension reduction of 60%. A further reduction in fiber dimensions (~80%) achieved by the treatment condition-75MN produced a CNF with ~6% solid content. The reduced fiber dimensions achieved by severe ball milling treatment, especially 75MC, and 75MN samples decreased the entangled structure of CNF and reduced the water holding capacity of hydrogel (Lasseuguette et al. 2008; Pääkkö et al. 2007; Salas et al. 2014)

The one-way ANOVA test confirmed that the CNF solid content was significantly different between different treatment methods and the control sample (see the supplementary document - Table S3). Furthermore, the multiple comparison test showed that the CNF solid contents from the treatments 15MC and 45MC including the control sample (0MC) were significantly different from the rest of the samples (75MC, 15MN, 45MN, and 75MN) (see the supplementary document - Fig. S3). Therefore, a short fiber length (<50 μm) with mild alkaline treated cellulose can produce consistent quality and high solid content CNF using a high-pressure homogenizer.

Dispersion stability

The dispersion stability of CNF depends on the surface charge density of CNF emulsion. The strong repulsive forces generated by electric charges of CNF emulsion in water prevented fibril agglomeration (Chami Khazraji and Robert 2013; Nishiyama 2018). The surface charges of CNF samples are usually measured and reported as zeta potential (mV). The observed mean zeta potentials of all CNF samples were close to 30 mV and were 60% higher than that of the Ref. sample as shown in Table 2. The higher electric charges of the cellulose chains indicated the higher Coulomb repulsive forces between cellulose molecules that prevented the agglomeration and improved the dispersion stability. When the zeta potential values are higher than the absolute value of 15 mV, the CNF suspensions in an aqueous

solution were considered stable (Dukhin and Goetz 1998; Khouri 2010; Mohaiyiddin et al. 2016). The dispersion of cellulose in water is due to the interaction of cellulose chains and water molecules through electrostatic forces. The electrostatic forces appear between hydrogen atoms with δ + charge and a cellulose chain carrying δ- charge (Chami Khazraji and Robert 2013; Rizzato et al. 2010). The one-way ANOVA test on the zeta potential of CNF from different treatments confirmed that there were no significant differences among the treatments and the control sample (see the supplementary document - Table S4). The increased fiber surface area during the ball milling treatment generated higher surface changes on the CNF hydrogel with stable dispersion stability (Jiang and Hsieh 2013). Therefore, short and uniform fiber dimensions facilitated effective fibrillation of cellulose fibers to produce highly dispersible CNF hydrogel.

FTIR analysis

The chemical structure of all the CNF samples was verified by Fourier-transformed infrared (FTIR) spectra as shown in Fig. 3. There were no significant changes in the FTIR spectra among all CNF samples. Further, the absorbance intensity peaks for all manufactured CNF were the same as peaks for cellulose reported in the literature and the Ref. sample (Abraham et al. 2011; Kasa et al. 2017; Lani et al. 2014). The cellulose fiber pretreatments helped to liberate fibrils with reduced dimension by breaking the inter and intramolecular hydrogen bonds as reported by Nuruddin et al. 2016 (Nuruddin et al. 2016).

The characteristic peak with a broad region between 3,500 - 3,200 cm^{-1} corresponded to O-H groups' stretching vibrations. The stretching frequency at 2899 cm^{-1} was due to -CH groups. The mild peak around 1646 cm^{-1} frequency was attributed to the bending of -OH groups in absorbed water. The spectra peak of -CH_2- and -C-H groups were indicated by 1430 and 1320 cm^{-1} vibration frequencies (Abraham et al. 2011; Kasa et al. 2017; Lani et al. 2014). The vibration frequencies of C-O stretching and C-OH have appeared in spectra at 1151 and 1112 cm^{-1}. The peak at 1043 and 896 cm^{-1} were attributed to the C-O-C skeletal vibration of pyranose rings and the deformation of β-glycosidic linkages respectively (Zhao et al. 2017).

Crystalline structure

The crystallinity of CNF samples was studied from X-ray diffractograms (XRD) as shown in Fig. 4. It shows the peaks at 2θ = 17 to 18° and 26 to 27° corresponding to cellulose crystallographic planes 1 0 1 and 0 0 2 defined by International Center for Diffraction Data – ICDD (Morais et al. 2013b). It also implies that the cellulose type I did not change into type II allomorph by any of the treatment processes.

The one-way ANOVA and multiple comparison tests inferred no significant differences among the crystallinity index of all treated CNF, control, and Ref. samples (see the supplementary document - Table and Fig. S5). The crystallinity index was about 72% for control (0MC), Ref. and certain treated samples (15MC, 45MC, and 15MN). It was slightly increased by up to 5% for the treated samples- 75MC, 45MN and 75MN. The impact and shear forces applied over cellulose fibers during ball milling were effective to

isolate fibers from the bundle and to reduce amorphous regions without affecting the crystalline region (Nuruddin et al. 2016; Yu and Wu 2011; Zhang et al. 2015). The NaOH treated samples showed a slightly increased crystallinity index than that of the CMC dispersed samples. The ball milling of NaOH treated fibers exhibited a marginal reduction in the amorphous regions of cellulose causing a slight increase in crystallinity index (Fattahi Meyabadi et al. 2014; Zhao et al. 2006). However, the effect of ball milling was not severe to reduce the crystalline region as reported elsewhere (Amidon and Houghton 1995; Zhao et al. 2006; Lee 2016; Lee et al. 2018).

Table 2

The total solid content, zeta potential, and the crystallinity index of various pretreated CNF samples[1]

Sample ID	Solid content (%)[b]	Zeta potential (mV)[c]	Crystallinity Index (%)[d]
0MC	4.2±0.5*	29±2#	72±1@
15MC	3.9±0.1*	29±2#	73±8@
45MC	4.1±0.3*	30±4#	73±1@
75MC	5.5±0.2**	30±3#	75±3@
15MN	5.3±0.6**	31±3#	73±1@
45MN	5.3±0.5**	32±2#	76±4@
75MN	5.7±0.7**	29±3#	75±6@
Ref.[a]	3.0±1.0***	18±2##	73±1@
[a]Ref. – The reference CNF sample was obtained from the University of Maine			
[b]Data presented after the symbol – "±" are standard deviations with n = 9			
[c]Data presented after the symbol – "±" are standard deviations with n = 20			
[d]Data presented after the symbol – "±" are standard deviations with n = 3			
[1]Mean values under each column with the same type of symbols are not significantly different at a 5% confidence interval			

Morphological Structure

The SEM images of CNF film samples were used to estimate the average width of cellulose fibrils as shown in Fig. 5. A strong cellulose microstructure network with entangled fibrils was observed in the SEM images. The surface morphology of the fibrils was smooth in all the samples. The CMC dispersion, NaOH swelling, and ball milling treatments affected the CNF fibril width. The control CNF sample (0MC) had an

average fibrils width of about 43±19 nm. The average width of fibrils from 15MC and 45MC samples was in the range of 20 to 30 nm and was less than 20 nm for the rest of the samples (75MC, 15MN, 45MN, and 75MN). The reduction of cellulose fiber width and length to less than ~5 and 50 μm by pretreatment methods caused smaller fibril width in 75MC, 15MN, 45MN, and 75MN CNF samples.

A one-way ANOVA analysis of fibril width on various pretreatment methods indicated that there was a significant difference between the treated and the control CNF samples (see the supplementary document - Table S6). It was also found from multiple comparison tests that the mean fibril width was significantly different from all pretreated samples and the control and Ref. samples. The mean fibril width in CNF samples-15MC and 45MC were also significantly different from the rest of the samples (see the supplementary document - Fig. S6). The multi-comparison analysis confirmed that the reduction in fibril dimension by the pretreatment methods such as CMC dispersion, NaOH swelling, and ball milling could significantly influence CNF fibril width. The impact and shear forces on cellulose fibers by the collision of balls broke the inter and intramolecular hydrogen bonds and reduced their dimensions during pretreatment. The consecutive pressurized flow of pretreated cellulose through nozzle ruptured the cell wall of the microfibril bundles and liberated nanostructured fibrils with less than 30 nm of CNF from a high-pressure homogenizer (Hernández-Varela et al. 2021; Mattonai et al. 2018; Tarrés et al. 2020).

Thermal degradation analysis

The thermal degradation behavior of CNF was studied from the thermogravimetric (TG) and derivative thermogravimetric (DTG) curves presented in Fig. 6. In all samples, an initial weight loss of 5% was observed between 40 to 100°C due to absorbed moisture. The second stage of weight loss was due to the thermal degradation of cellulose. The weight loss varied between 45 to 60% for different pretreatment methods. It occurred between 313 to 370°C for all samples. The third stage of degradation continued beyond 370°C and left residual masses after degradation at 650°C. The pretreatment method by NaOH swelling and 15 and 45 min ball milling produced loosely packed nanofibrils to leave reduced residual masses (Peng et al. 2013).

The DTG curves showed the peak degradation temperature at 340°C for control CNF (control sample-0MC) and 350°C for all CNF produced by the combination of pretreatment methods followed by homogenization as reported elsewhere (Abraham et al. 2011; Alvarez and Vázquez 2006; Yang et al. 2007). Further, the improved thermal stability revealed the improved cellulose fibrillation due to pretreatment methods (Luo and Wang 2017). The NaOH pretreated CNF had a slightly increased thermal stability than that of CMC pretreated CNF due to ruptured amorphous region and liberated small-size fibrils (Lee et al. 2018).

Tensile strength

Figure 7 shows the comparison of maximum tensile stress and Young's modulus all pretreated CNF, control, and Ref. films. The deformation behavior of all CNF films was linear at a low strain rate of 1 to

2% and the maximum tensile stress was observed before the breaking point as reported in the literature (Chun et al. 2011; Xu et al. 2018). The CMC and NaOH treatments with different ball milling times affected the tensile properties of films. The maximum tensile stress and Young's modulus of the control CNF sample were 58±6 MPa and 5±1 GPa, respectively. The maximum tensile stress of CMC dispersion-ball mill treated CNF films was 65 to 73% more than that of control films. The 75MC CNF samples showed the maximum tensile stress of 99±5 MPa. The maximum tensile stress of NaOH-ball mill pretreated CNF samples were 39 to 72% more than that of control films. The 75MN CNF samples exhibited the highest tensile strength of 105±14 MPa. The maximum tensile stress of CNF manufactured with pretreatment methods was within the range of 80 to 105 MPa as reported elsewhere (Bruce et al. 2005; Das et al. 2017; Leitner et al. 2007; Zimmermann et al. 2010).

Young's modulus for all the pretreated samples was about 71 to 85% more than that of control films. The CNF manufactured from CMC/NaOH treatment with 75min ball milling pretreatment (75MC and 75MN) had the maximum Young's modulus of 8 GPa. Moreover, the CNF samples manufactured from all the pretreatment methods showed about 30 and 15% higher tensile strength and Young's modulus than that of the Ref. sample.

The increased tensile properties of pretreated CNF samples indicated the presence of rigid nanofibril network structure in CNF films. The CNF fibrilization process also increased the surface area of fibers for hydrogen bonding. The hydrogen-bonded fibril network with reduced porosities increased the tensile strength of films prepared from pretreated CNF. It was evident from SEM images that a combination of CMC dispersion/NaOH swelling and ball milling effectively liberated nanostructured fibrils having a width up to 30 nm. The fibrils with reduced width exposed more hydroxyl groups for hydrogen bonding and enhanced entanglement of the network to resist deformation by higher tensile loading. The loosely packed network due to larger width fibrils resulted in lower tensile strength in control samples.

Conclusions

The cellulose powder treated by CMC dispersion with 75 min ball milling and NaOH swelling with 15-75 min ball milling achieved more than 80% fiber dimension reduction. This reduction in cellulose fiber dimensions by various pretreatment methods increased the CNF solid content by up to 6%. It also enhanced the dispersion abilities and prevented the clogging of cellulose micro bundles during the homogenization process. Among the pretreatment methods, the NaOH-15 min ball mill treatment was the most effective pretreatment that used the least ball milling time for the larger fiber size reductions. However, the CMC/NaOH treatment with the longest ball milling time of 75 min produced the highest solid content CNF during high-pressure homogenization. The pretreatment method did not influence the chemical structure and dispersion abilities. The crystallinity was increased by 4 to 5% for CMC dispersion with 75 min ball milling and NaOH swelling with 45 and 75 min ball milling pretreatments. The thermal degradation study revealed a marginal improvement in thermal stability of all CNF samples. The tensile strength of CNF films manufactured from all pretreated samples was between 80 and 105 MPa. Overall,

short cellulose fibers with mild alkaline pretreatment can produce consistent quality and highly dispersible CNF hydrogel with high solid content for industrial applications.

Declarations

Acknowledgments

The authors acknowledge Dr. Jason Locklin, Dr. Eric Freeman, Dr. Gajanan Bhat, Dr. Rakesh K. Singh, Dr. Paul A Schroeder, Dr. Eric Formo, Dr. Raha Saremi, Ms. Michelle Massoud Makhoul-Mansour, Mr. Matthew Dean Seivert, Ms. Shruti Sharma, Ms. Smriti Dilliwar, Ms. Anh Hoang Truc Dang and Mr. Arjun Kumar Kotapalli of University of Georgia (UGA) for extending their support in the experimental study.

References

1. Abdul Khalil HPS et al. (2016) A review on nanocellulosic fibers as new material for sustainable packaging: Process and applications. Renew Sust Energ Rev 64:823-836. doi:https://doi.org/10.1016/j.rser.2016.06.072.
2. Abitbol T et al. (2016) Nanocellulose, a tiny fiber with huge applications. Curr Opin Biotechnol 39:76-88. doi:https://doi.org/10.1016/j.copbio.2016.01.002.
3. Abraham E, Deepa B, Pothan LA, Jacob M, Thomas S, Cvelbar U, Anandjiwala R (2011) Extraction of nanocellulose fibrils from lignocellulosic fibers: A novel approach. Carbohydr Polym 86:1468-1475. doi:https://doi.org/10.1016/j.carbpol.2011.06.034.
4. Adsul MG, Ghule JE, Shaikh H, Singh R, Bastawde KB, Gokhale DV, Varma AJ (2005) Enzymatic hydrolysis of delignified bagasse polysaccharides. Carbohydr Polym 62:6-10. doi:https://doi.org/10.1016/j.carbpol.2005.07.010.
5. Albornoz-Palma G, Ching D, Valerio O, Mendonça RT, Pereira M (2020) Effect of lignin and hemicellulose on the properties of lignocellulose nanofibril suspensions. Cellulose 27:10631-10647. doi:https://doi.org/10.1007/s10570-020-03304-5.
6. Alle M, Bandi R, Lee S-H, Kim J-C (2020) Recent trends in isolation of cellulose nanocrystals and nanofibrils from various forest wood and nonwood products and their application. In: Nanomaterials for agriculture and forestry applications. Elsevier, pp 41-80. doi:https://doi.org/10.1016/B978-0-12-817852-2.00003-2
7. Alvarez VA, Vázquez A (2006) Influence of fiber chemical modification procedure on the mechanical properties and water absorption of MaterBi-Y/sisal fiber composites. Compos - A: Appl Sci Manuf 37:1672-1680. doi:https://doi.org/10.1016/j.compositesa.2005.10.005.
8. Amidon GE, Houghton ME (1995) The effect of moisture on the mechanical and powder flow properties of microcrystalline. Pharm Res 12:923-929. doi:10.1023/A:1016233725612.
9. Arantes V, Dias IKR, Berto GL, Pereira B, Marotti BS, Nogueira CFO (2020) The current status of the enzyme-mediated isolation and functionalization of nano cellulose: production, properties, techno-

economics, and opportunities. Cellulose 27:10571-10630. doi:10.1007/s10570-020-03332-1.

10. Arvidsson R, Nguyen D, Svanström M (2015) Life cycle assessment of cellulose nanofibrils production by mechanical treatment and two different pretreatment processes. Environ Sci Technol 49:6881-6890. doi:10.1021/acs.est.5b00888.
11. Avolio R, Bonadies I, Capitani D, Errico ME, Gentile G, Avella M (2012) A multitechnique approach to assess the effect of ball milling on cellulose. Carbohydr Polym 87:265-273. doi:https://doi.org/10.1016/j.carbpol.2011.07.047.
12. Bai F-W, Yang S, Ho NWY (2019) Fuel ethanol production from lignocellulosic biomass. In: Moo-Young M (ed) Comprehensive biotechnology (Third Edition). Pergamon, Oxford, pp 49-65. doi:https://doi.org/10.1016/B978-0-444-64046-8.00150-6
13. Bilodeau MA, Paradis MA (2018) High efficiency production of nanofibrillated cellulose. 9,988,762.
14. Brigham C (2018) Biopolymers: Biodegradable alternatives to traditional plastics. In: Török B, Dransfield T (eds) Green chemistry. Elsevier, pp 753-770. doi:https://doi.org/10.1016/B978-0-12-809270-5.00027-3
15. Bruce DM, Hobson RN, Farrent JW, Hepworth DG (2005) High-performance composites from low-cost plant primary cell walls. Compos - A: Appl Sci Manuf 36:1486-1493. doi:https://doi.org/10.1016/j.compositesa.2005.03.008.
16. Cai J, Zhang L (2005) Rapid dissolution of cellulose in LiOH/urea and NaOH/urea aqueous solutions. Macromol Biosci 5:539-548 doi:https://doi.org/10.1002/mabi.200400222
17. Chami Khazraji A, Robert S (2013) Self-assembly and intermolecular forces when cellulose and water interact using molecular modeling. J of Nanomater 2013:745979. doi:10.1155/2013/745979.
18. Cheng L, Zhang D, Gu Z, Li Z, Hong Y, Li C (2018) Preparation of acetylated nanofibrillated cellulose from corn stalk microcrystalline cellulose and its reinforcing effect on starch films. Int J of Biol Macromol 111:959-966. doi:https://doi.org/10.1016/j.ijbiomac.2018.01.056.
19. Chirayil CJ, Mathew L, Thomas S (2014) Review of recent research in nano cellulose preparation from different lignocellulosic fibers. Rev Adv Mater Sci 37:20-28.
20. Chun S-J, Lee S-Y, Doh G-H, Lee S, Kim JH (2011) Preparation of ultrastrength nanopapers using cellulose nanofibrils. J Ind Eng Chem 17:521-526 doi:https://doi.org/10.1016/j.jiec.2010.10.022
21. Cowie J, Bilek ET, Wegner TH, Shatkin JA (2014) Market projections of cellulose nanomaterial-enabled products-Part 2: Volume estimates. Tappi J 13:57-69
22. Das O, Kim NK, Bhattacharyya D (2017) 16 - The mechanics of biocomposites. In: Ambrosio L (ed) Biomedical composites (Second edition). Woodhead publishing, pp 375-411. doi:https://doi.org/10.1016/B978-0-08-100752-5.00017-2.
23. Dukhin AS, Goetz PJ (1998) Characterization of aggregation phenomena by means of acoustic and electroacoustic spectroscopy. Colloids Surf A Physicochem Eng Asp 144:49-58 doi:https://doi.org/10.1016/S0927-7757(98)00565-2

24. Fattahi Meyabadi T, Dadashian F, Mir Mohamad Sadeghi G, Ebrahimi Zanjani Asl H (2014) Spherical cellulose nanoparticles preparation from waste cotton using a green method. Powder Technol 261:232-240 doi:https://doi.org/10.1016/j.powtec.2014.04.039
25. Fras-Zemljič L, Stenius P, Laine J, Stana-Kleinschek K (2006) The effect of adsorbed carboxymethyl cellulose on the cotton fibre adsorption capacity for surfactant. Cellulose 13:655-663. doi:10.1007/s10570-006-9071-2.
26. Gu H, Reiner R, Bergman R, Rudie (2015) A LCA study for pilot scale production of cellulose nano crystals (CNC) from wood pulp. In: Proceedings from the LCA XV conference, 2015. pp 33-42.
27. Hai LV, Park HJ, Seo YB (2013) Effect of PFI mill and valley beater refining on cellulose degree of polymerization, alpha cellulose contents, and crystallinity of wood and cotton fibers. J of Korea TAPPI 45:27-33.
28. Havstad MR (2020) Biodegradable plastics. In: Letcher TM (ed) Plastic waste and recycling. Academic press, pp 97-129. doi:https://doi.org/10.1016/B978-0-12-817880-5.00005-0.
29. Hernández-Varela JD, Chanona-Pérez JJ, Calderón Benavides HA, Cervantes Sodi F, Vicente-Flores M (2021) Effect of ball milling on cellulose nanoparticles structure obtained from garlic and agave waste. Carbohydr Polym 255:117347. doi:https://doi.org/10.1016/j.carbpol.2020.117347
30. Ioelovich M, Morag E (2011) Effect of cellulose structure on enzymatic hydrolysis. Bioresources 6:2818-2835.
31. Iwamoto S, Nakagaito AN, Yano H (2007) Nano-fibrillation of pulp fibers for the processing of transparent nanocomposites. Appl Phys A 89:461-466. doi:10.1007/s00339-007-4175-6.
32. Iwamoto S, Nakagaito AN, Yano H, Nogi M (2005) Optically transparent composites reinforced with plant fiber-based nanofibers. Appl Phys A 81:1109-1112. doi:10.1007/s00339-005-3316-z.
33. Jiang F, Hsieh Y-L (2013) Chemically and mechanically isolated nanocellulose and their self-assembled structures Carbohydr Polym 95:32-40 doi:https://doi.org/10.1016/j.carbpol.2013.02.022
34. Kasa SN, Omar MF, Abdullah M, Ismail IN, Ting SS, Vizureanu P (2017) Effect of unmodified and modified nanocrystalline cellulose reinforced polylactic acid (PLA) polymer prepared by solvent casting method morphology, mechanical and thermal properties. Mater Plast 54:91-97.
35. Kępa K, Chaléat CM, Amiralian N, Batchelor W, Grøndahl L, Martin DJ (2019) Evaluation of properties and specific energy consumption of spinifex-derived lignocellulose fibers produced using different mechanical processes. Cellulose 26:6555-6569. doi:10.1007/s10570-019-02567-x.
36. Khouri S (2010) Experimental characterization and theoretical calculations of responsive polymeric systems. Dissertation, University of Waterloo.
37. Klemm D, Kramer F, Moritz S, Lindström T, Ankerfors M, Gray D, Dorris A (2011) Nanocelluloses: a new family of nature-based materials. Angew Chem Int Ed 50:5438-5466.
38. Laine (2000) Studies on topochemical modification of cellulosic fibres: Part 1. Chemical conditions for the attachment of carboxymethyl cellulose onto fibres.Nord Pulp Paper Res J 15:520-526. doi:10.3183/npprj-2000-15-05-p520-526.

39. Lani N, Ngadi N, Johari A, Jusoh M (2014) Isolation, characterization, and application of nanocellulose from oil palm empty fruit bunch fiber as nanocomposites. J Nanomater 2014.
40. Lasseuguette E, Roux D, Nishiyama Y (2008) Rheological properties of microfibrillar suspension of TEMPO-oxidized pulp. Cellulose 15:425-433.
41. Lawoko M, Henriksson G, Gellerstedt G (2006) Characterisation of lignin-carbohydrate complexes (LCCs) of spruce wood (Picea abies L.) isolated with two methods. Wood Res Technol 60:156-161. doi:doi:10.1515/HF.2006.025.
42. Lee H (2016) Preparation and characterization of cellulose nanofibrils using various pretreatment techniques. Dissertation, University of Georgia.
43. Lee H, Sundaram J, Zhu L, Zhao Y, Mani S (2018) Improved thermal stability of cellulose nanofibrils using low-concentration alkaline pretreatment. Carbohydr Polym 181:506-513. doi:https://doi.org/10.1016/j.carbpol.2017.08.119.
44. Leitner J, Hinterstoisser B, Wastyn M, Keckes J, Gindl W (2007) Sugar beet cellulose nanofibril-reinforced composites. Cellulose 14:419-425. doi:10.1007/s10570-007-9131-2.
45. Li F, Mascheroni E, Piergiovanni L (2015) The potential of nanocellulose in the packaging field: a review. Packag Technol Sci 28:475-508.
46. Li Q, McGinnis S, Sydnor C, Wong A, Renneckar S (2013) Nanocellulose life cycle assessment. ACS Sustain Chem Eng 1:919-928. doi:10.1021/sc4000225.
47. Liu L, Kong F (2019) Influence of nanocellulose on in vitro digestion of whey protein isolate. Carbohydr Polym 210:399-411. doi:https://doi.org/10.1016/j.carbpol.2019.01.071.
48. Lokanathan AR, Kontturi E, Linder MB, Rojas OJ, Ikkala O, Gröschel AH (2017) 9.19 - Nanocellulose-based materials in supramolecular chemistry. In: Atwood JL (ed) Comprehensive supramolecular chemistry II. Elsevier, Oxford, pp 351-364. doi:https://doi.org/10.1016/B978-0-12-409547-2.12531-4
49. Luo X, Wang X (2017) Preparation and characterization of nanocellulose fibers from NaOH/urea pretreatment of oil palm fibers. Bioresources 12:5826-5837.
50. Mattonai M, Pawcenis D, del Seppia S, Łojewska J, Ribechini E (2018) Effect of ball-milling on crystallinity index, degree of polymerization and thermal stability of cellulose. Bioresour Technol 270:270-277. doi:https://doi.org/10.1016/j.biortech.2018.09.029.
51. Mohaiyiddin MS et al. (2016) Characterization of nanocellulose recovery from Elaeis guineensis frond for sustainable development. Clean Technol Environ Policy 18:2503-2512. doi:10.1007/s10098-016-1191-2.
52. Moon RJ, Martini A, Nairn J, Simonsen J, Youngblood J (2011) Cellulose nanomaterials review: structure, properties and nanocomposites. Chem Soc Rev 40:3941-3994.
53. Morais JPS, de Freitas Rosa M, Nascimento LD, do Nascimento DM, Cassales AR (2013a) Extraction and characterization of nanocellulose structures from raw cotton linter. Carbohydr Polym 91:229-235.

54. Morais JPS, Rosa MdF, de Souza Filho MdsM, Nascimento LD, do Nascimento DM, Cassales AR (2013b) Extraction and characterization of nanocellulose structures from raw cotton linter. Carbohydr Polym 91:229-235. doi:https://doi.org/10.1016/j.carbpol.2012.08.010.
55. Nechyporchuk O, Pignon F, Belgacem MN (2015) Morphological properties of nanofibrillated cellulose produced using wet grinding as an ultimate fibrillation process. J Mater Sci 50:531-541. doi:10.1007/s10853-014-8609-1.
56. Nishiyama Y (2018) Molecular interactions in nanocellulose assembly. Philos Trans Royal Soc A 376:20170047. doi:doi:10.1098/rsta.2017.0047.
57. Nuruddin M, Hosur M, Uddin MJ, Baah D, Jeelani S (2016) A novel approach for extracting cellulose nanofibers from lignocellulosic biomass by ball milling combined with chemical treatment. J Appl Polym Sci 133. doi:https://doi.org/10.1002/app.42990.
58. Pääkkö M et al. (2007) Enzymatic hydrolysis combined with mechanical shearing and high-pressure homogenization for nanoscale cellulose fibrils and strong gels. Biomacromolecules 8:1934-1941.
59. Peng BL, Dhar N, Liu HL, Tam KC (2011) Chemistry and applications of nanocrystalline cellulose and its derivatives: A nanotechnology perspective. Can J Chem Eng 89:1191-1206. doi:https://doi.org/10.1002/cjce.20554.
60. Peng Y, Gardner DJ, Han Y, Kiziltas A, Cai Z, Tshabalala MA (2013) Influence of drying method on the material properties of nanocellulose I: thermostability and crystallinity. Cellulose 20:2379-2392. doi:10.1007/s10570-013-0019-z.
61. Pirich CL, Picheth GF, Fontes AM, Delgado-Aguilar M, Ramos LP (2020) Disruptive enzyme-based strategies to isolate nanocelluloses: a review. Cellulose 27:5457-5475. doi:10.1007/s10570-020-03185-8.
62. Rizzato S, Bergès J, Mason SA, Albinati A, Kozelka J (2010) Dispersion-driven hydrogen bonding: Predicted hydrogen bond between water and platinum(II) identified by neutron diffraction. Angew Chem Int Ed 49:7440-7443 doi:https://doi.org/10.1002/anie.201001892.
63. Saito T, Okita Y, Nge TT, Sugiyama J, Isogai A (2006) TEMPO-mediated oxidation of native cellulose: Microscopic analysis of fibrous fractions in the oxidized products. Carbohydr Polym 65:435-440. doi:https://doi.org/10.1016/j.carbpol.2006.01.034.
64. Salas C, Nypelö T, Rodriguez-Abreu C, Carrillo C, Rojas OJ (2014) Nanocellulose properties and applications in colloids and interfaces. Curr Opin Colloid Interface Sci 19:383-396. doi:https://doi.org/10.1016/j.cocis.2014.10.003.
65. Segal L, Creely JJ, Martin Jr A, Conrad C (1959) An empirical method for estimating the degree of crystallinity of native cellulose using the X-ray diffractometer. Text Res J 29:786-794.
66. Selvaraj T, Perumal V, Khor SF (2021) 13 - Non-metallic nanomaterial productions from natural resources. In: Gopinath SCB, Gang F (eds) Nanoparticles in analytical and medical devices. Elsevier, pp 247-276. doi:https://doi.org/10.1016/B978-0-12-821163-2.00013-3
67. Singh S, Wasewar KL, Kansal SK (2020) Chapter 10 - Low-cost adsorbents for removal of inorganic impurities from wastewater. In: Devi P, Singh P, Kansal SK (eds) Inorganic pollutants in water. Elsevier,

pp 173-203. doi:https://doi.org/10.1016/B978-0-12-818965-8.00010-X

68. Stelte W, Sanadi AR (2009) Preparation and characterization of cellulose nanofibers from two commercial hardwood and softwood pulps. Ind Eng Chem Res 48:11211-11219.
69. TAPPI (2017) Standard terms and their definition for cellulose nanomaterial. WI 3021. https://www.tappi.org/content/hide/draft3.pdf. Accessed 1 June 2021
70. Tarrés Q, Oliver-Ortega H, Boufi S, Àngels Pèlach M, Delgado-Aguilar M, Mutjé P (2020) Evaluation of the fibrillation method on lignocellulosic nanofibers production from eucalyptus sawdust: A comparative study between high-pressure homogenization and grinding. Int J Biol Macromol 145:1199-1207. doi:https://doi.org/10.1016/j.ijbiomac.2019.10.046.
71. Turbak A, Snyder F, Sandberg K (1983) Microfibrillated Cellulose. U.S. Patent No. 4,374,702 .
72. Vanderghem C, Jacquet N, Danthine S, Blecker C, Paquot M (2012) Effect of physicochemical characteristics of cellulosic substrates on enzymatic hydrolysis by heans of a multi-stage process for cellobiose production. Appl Biochem Biotechnol 166:1423-1432. doi:10.1007/s12010-011-9535-1.
73. Xu J, Krietemeyer EF, Boddu VM, Liu SX, Liu W-C (2018) Production and characterization of cellulose nanofibril (CNF) from agricultural waste corn stover. Carbohydr Polym 192:202-207 doi:https://doi.org/10.1016/j.carbpol.2018.03.017
74. Yang H, Yan R, Chen H, Lee DH, Zheng C (2007) Characteristics of hemicellulose, cellulose and lignin pyrolysis. Fuel 86:1781-1788. doi:https://doi.org/10.1016/j.fuel.2006.12.013.
75. Yu Y, Wu H (2011) Effect of ball milling on the hydrolysis of microcrystalline cellulose in hot-compressed water. AIChE Journal 57:793-800. doi:https://doi.org/10.1002/aic.12288.
76. Zhang L, Tsuzuki T, Wang X (2015) Preparation of cellulose nanofiber from softwood pulp by ball milling. Cellulose 22:1729-1741.
77. Zhang Y, Nypelö T, Salas C, Arboleda J, Hoeger IC, Rojas OJ (2013) Cellulose nanofibrils. J Renew Mater 1:195-211. doi:10.7569/JRM.2013.634115.
78. Zhao H, Kwak JH, Wang Y, Franz JA, White JM, Holladay JE (2006) Effects of crystallinity on dilute acid hydrolysis of cellulose by cellulose ball-milling study. Energy Fuels 20:807-811. doi:10.1021/ef050319a.
79. Zhao Y, Moser C, Lindström ME, Henriksson G, Li J (2017) Cellulose Nanofibers from Softwood, Hardwood, and Tunicate: Preparation–Structure–Film Performance Interrelation. ACS Appl Mater Interfaces 9:13508-13519. doi:10.1021/acsami.7b01738.
80. Zimmermann T, Bordeanu N, Strub E (2010) Properties of nanofibrillated cellulose from different raw materials and its reinforcement potential. Carbohydr Polym 79:1086-1093. doi:https://doi.org/10.1016/j.carbpol.2009.10.045.

Figures

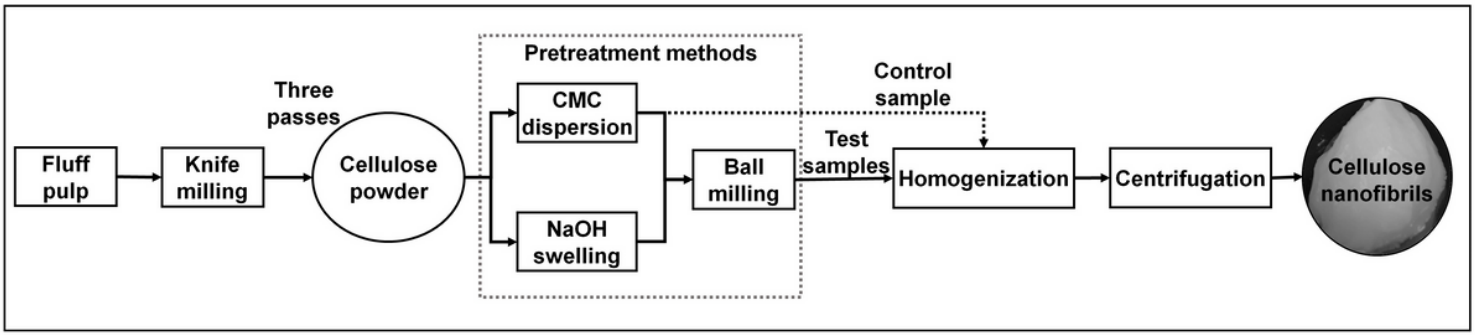

Figure 1

CNF production from pretreated cellulose powder

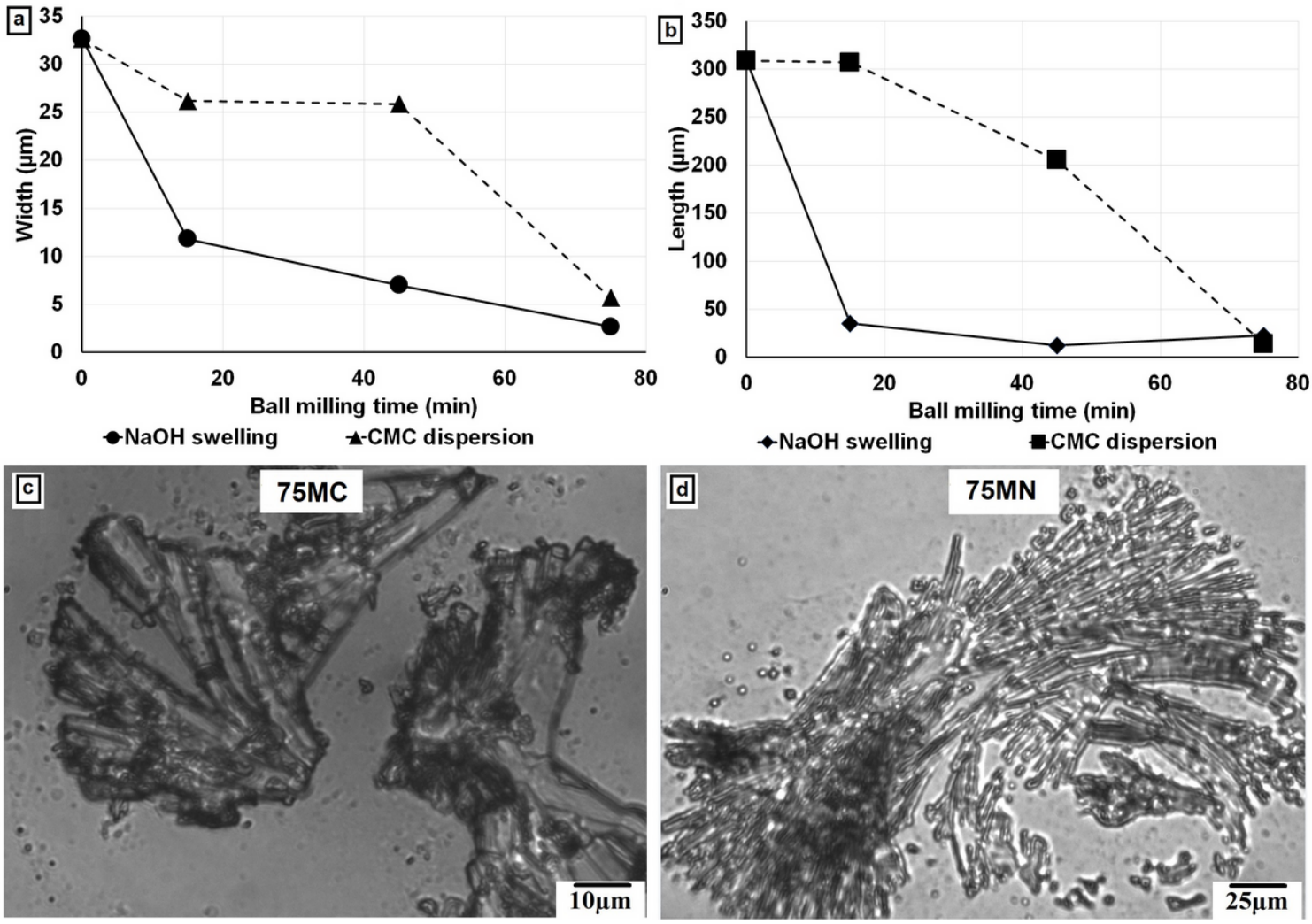

Figure 2

Fiber dimensions and optical microscope images of ball mill treated cellulose fibers. **a** Comparison of cellulose fiber width to different pretreatment conditions. **b** Comparison of cellulose fiber length to different pretreatment conditions. **c** Optical microscope image of a cellulose fiber after CMC dispersion-

75 min ball milling pretreatment. **d** Optical microscope image of a cellulose fiber after NaOH swelling-75 min ball milling pretreatment.

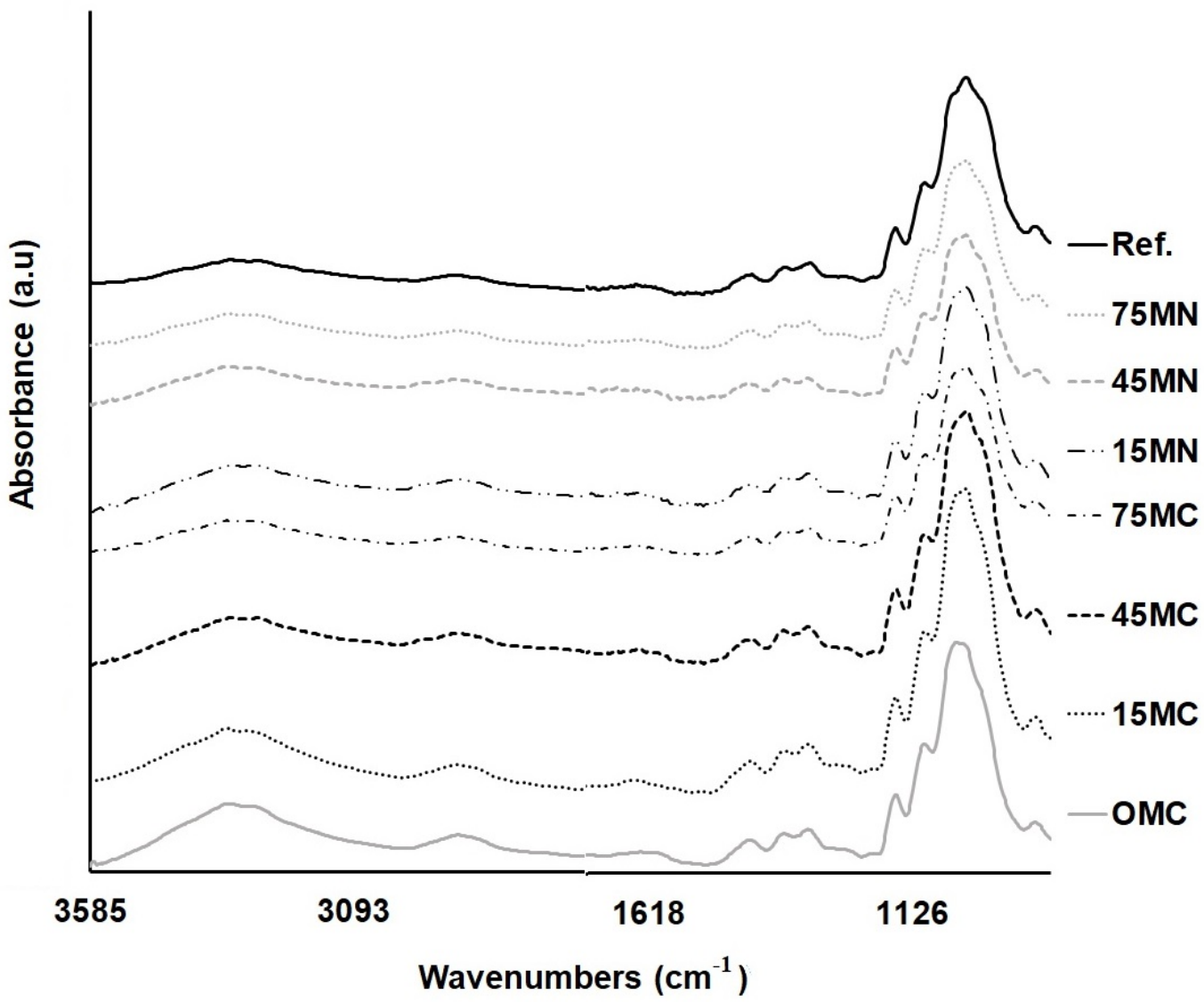

Figure 3

FTIR spectra of CNF manufactured by different treatment methods

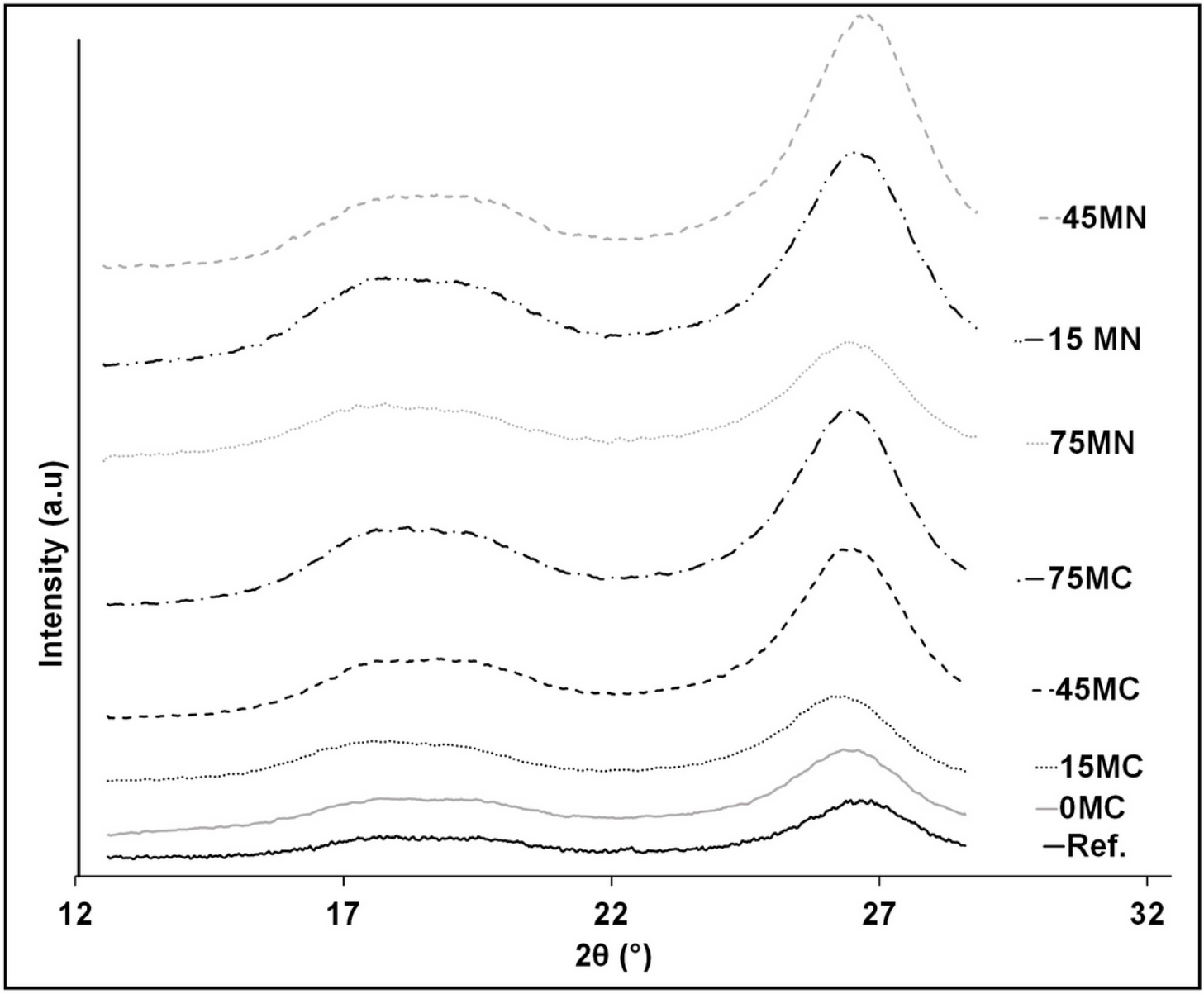

Figure 4

XRD curves of CNF manufactured by different treatment methods

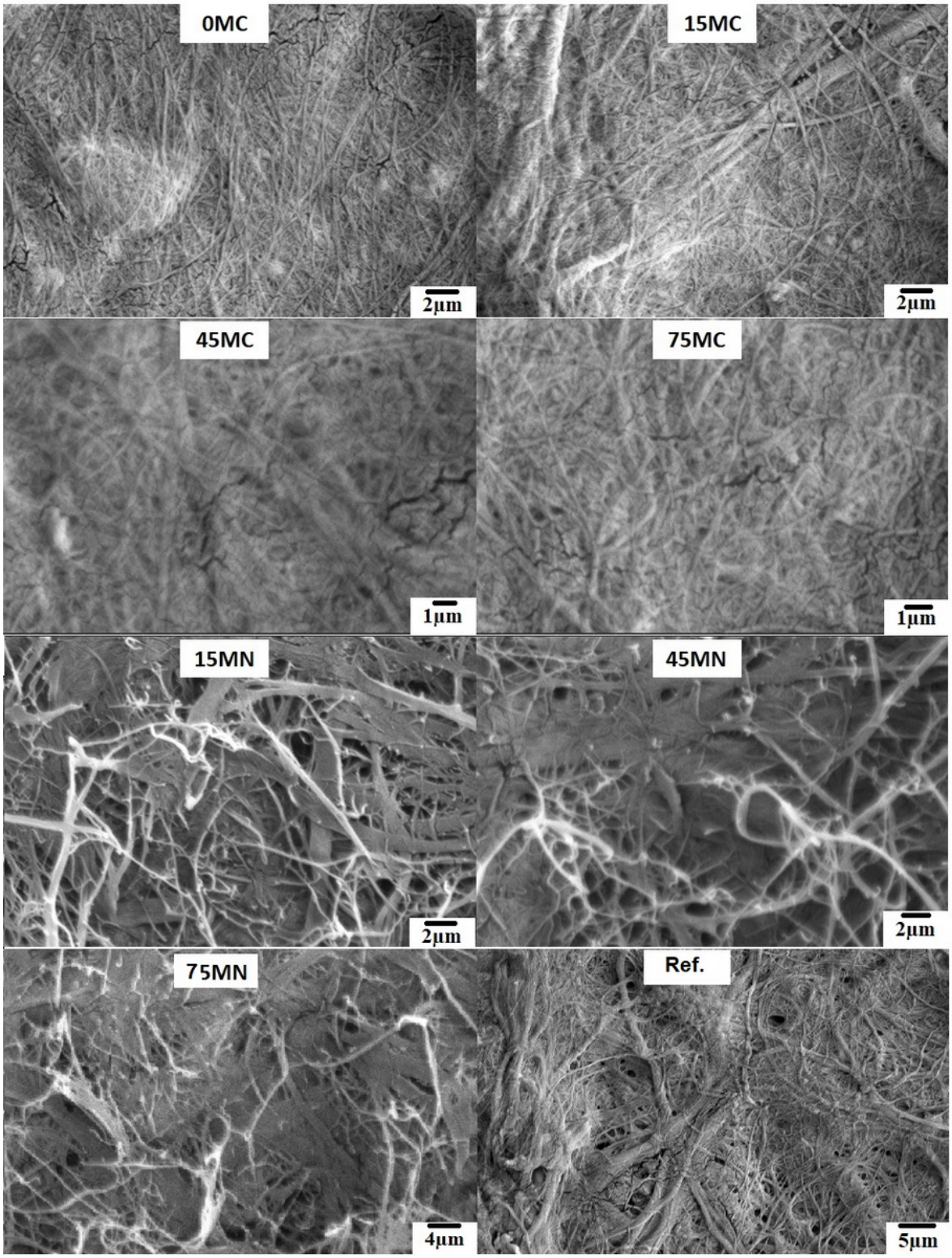

Figure 5

SEM images of CNF manufactured by different treatment methods and Ref. sample

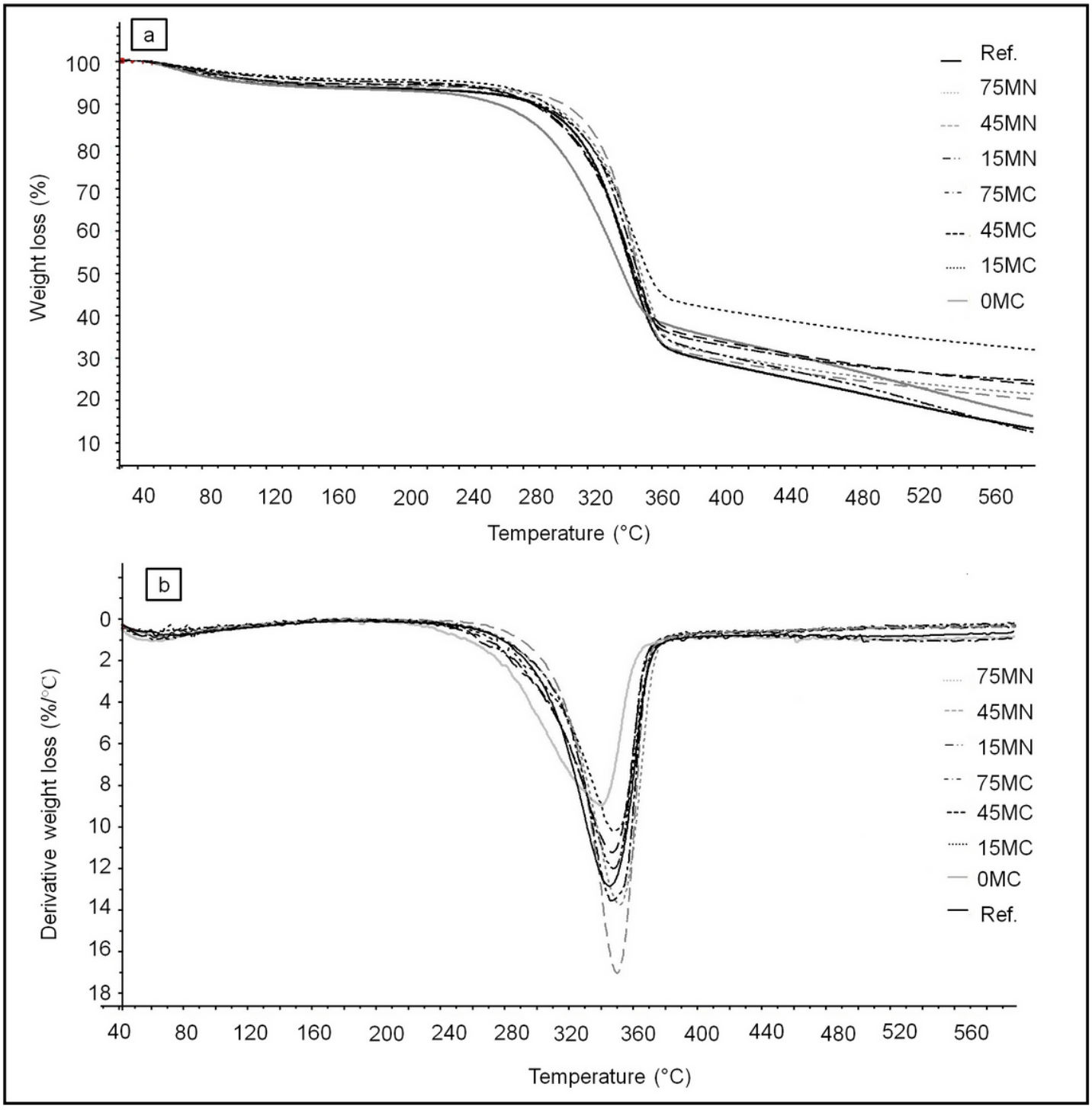

Figure 6

Thermograms of CNF a) TG curves b) DTG curves

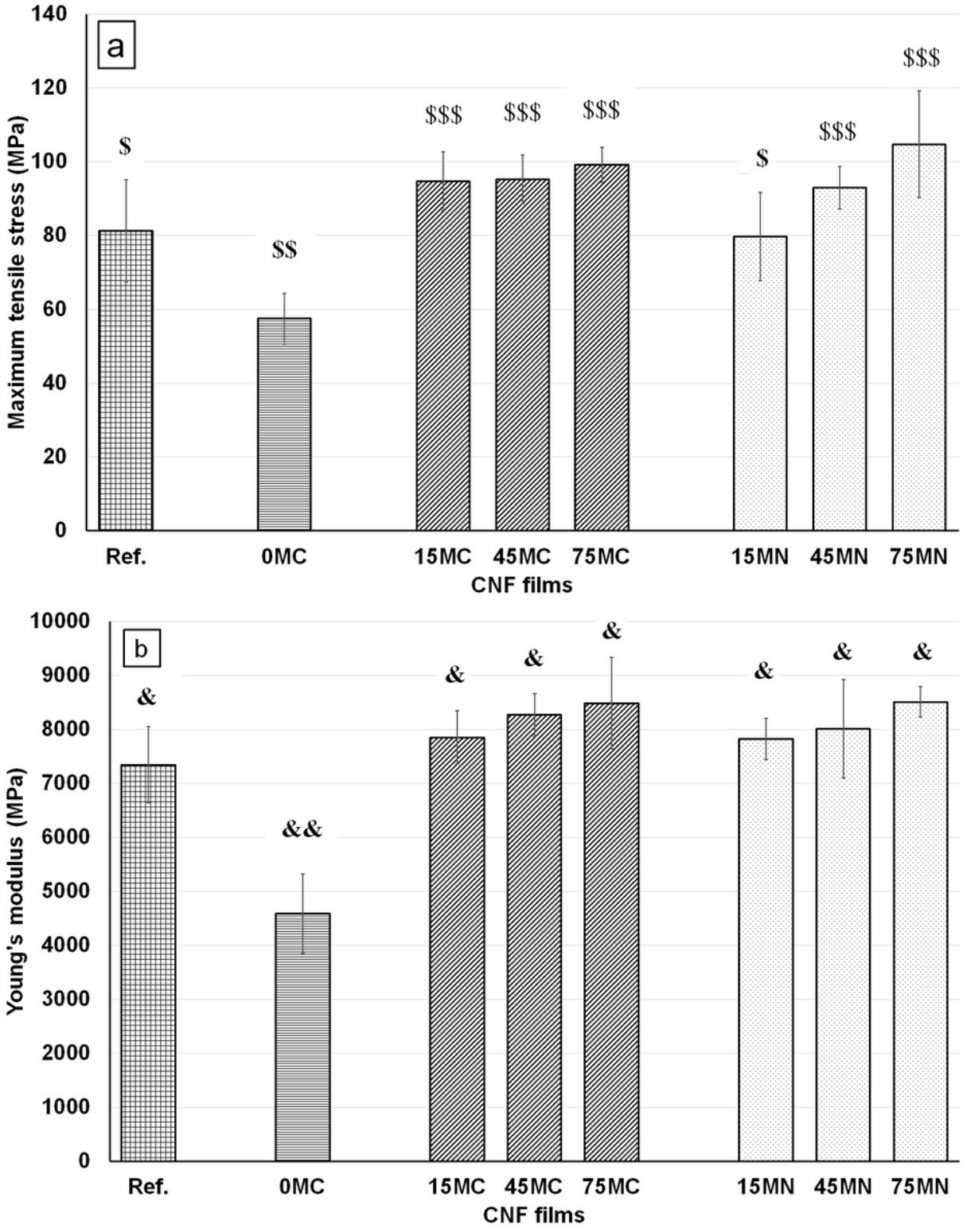

Figure 7

Comparison of tensile properties of Ref. and manufactured CNF films. **a** Tensile strength. **b** Young's modulus. Note: Mean values of tensile strength and Young's modulus marked by the same type of symbols in the columns are not significantly different at a 5% confidence interval.

Supplementary Files

This is a list of supplementary files associated with this preprint. Click to download.

- SupplementaryInformationSI.docx